Supplemental Material for "Magnetic helicity and the evolution of decaying magnetohydrodynamic turbulence"

Arjun Berera and Moritz Linkmann
SUPA, School of Physics and Astronomy, University of Edinburgh, UK

In this supplemental material we provide details of our investigation of reverse spectral transfers in magnetohydrodynamic turbulence, such as verification of our code and further tests of our results.

I. INTRODUCTION

In the paper [1] we conducted direct numerical simulations (DNS) of incompressible magnetohydrodynamic (MHD) turbulence without an imposed guide field. The MHD equations for incompressible flow are

$$\partial_t \boldsymbol{u} = -\frac{1}{\rho}\nabla P - (\boldsymbol{u}\cdot\nabla)\boldsymbol{u} + \frac{1}{\rho}(\nabla\times\boldsymbol{b})\times\boldsymbol{b} + \nu\Delta\boldsymbol{u} \ , \tag{1}$$

$$\partial_t \boldsymbol{b} = (\boldsymbol{b}\cdot\nabla)\boldsymbol{u} - (\boldsymbol{u}\cdot\nabla)\boldsymbol{b} + \eta\Delta\boldsymbol{b} \ , \tag{2}$$

$$\nabla\cdot\boldsymbol{u} = 0 \ \text{ and } \ \nabla\cdot\boldsymbol{b} = 0 \ , \tag{3}$$

where $\boldsymbol{u}$ denotes the velocity field, $\boldsymbol{b}$ the magnetic induction expressed in Alfvén units, ν the kinematic viscosity, η the resistivity, P the pressure and $\rho = 1$ the density.

We presented ensemble averaged data showing reverse spectral transfer (RST) of magnetic helicity and measured decay exponents for initially maximally helical magnetic fields. In a particular set of simulations we decoupled the momentum equation (1) from the induction equation (2) and showed that the inverse cascade of magnetic energy persists, while the reverse spectral transfer of magnetic helicity disappears in the decoupled system, provided the initial velocity field was nonhelical.

Details of our simulations can be found in Table I, where we specify values for Reynolds numbers, resolution, diffusivities, runtime t_{max}, ensemble size and wavenumber k_0 at which we set the peaks of the initial spectra.

II. VERIFICATION OF DNS CODE

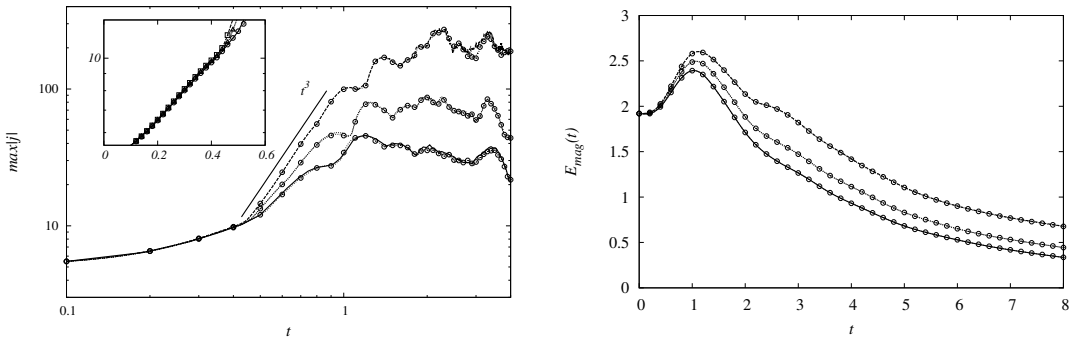
The 3D Orszag-Tang vortex was used for comparison against results by Mininni, Pouquet and Montgomery [2] and Morales, Leroy, Bos and Schneider [3]. The initial conditions are

$$\begin{aligned}\boldsymbol{u} &= (-2\sin y,\ 2\sin x,\ 0) \ , \\ \boldsymbol{b} &= \beta(-2\sin 2y + \sin z,\ 2\sin x + \sin z,\ \sin x + \sin y) \ ,\end{aligned} \tag{4}$$

where $\beta = 0.8$ has been chosen according to [2, 3]. We calculate the total dissipation

$$\varepsilon_{tot}(t) = \nu\langle\boldsymbol{\omega}^2\rangle + \eta\langle\boldsymbol{j}^2\rangle \ , \tag{5}$$

and the maximum of the current density in real space $\max|\boldsymbol{j}|$. We used the same number of grid points and diffusivities as [3], that is $\nu = \eta = 0.01$ on 64^3 points, $\nu = \eta = 0.005$ on 128^3 points and $\nu = \eta = 0.001$ on 256^3 points. Our results are in agreement with both above mentioned sources. The maximum of the current density shows Reynolds number independent exponential growth until $t = 0.4$, in agreement with Morales *et al.* , while Mininni *et al.* observe exponential growth up to $t = 0.6$. After this initial period we observe algebraic growth $\sim t^3$ in agreement with



(a)Evolution of the maximal current density (b)Magnetic energy

FIG. 1. Comparison to Morales *et al.* The symbols refer to our DNS, the lines to DNS by Morales *et al.*

both sources. With increasing Reynolds number the temporal maxima of $\max|\mathbf{j}|$ are achieved at later times, also in agreement with both sources. Our data shows very good agreement to a dataset obtained from Morales *et al.* [3], see Fig. 1.

III. INERTIAL RANGE PROPERTIES FOR THE FULL MHD EQUATIONS.

Figure 2 shows magnetic helicity, magnetic energy and kinetic energy spectra shortly after the onset of power-law decay (that is, at $t = 1.3t_0$) for the largest Reynolds number run H11. The magnetic helicity spectra have been multiplied by the wavenumber k for dimensional reasons, and have been shifted downwards in the figure to facilitate visual analysis. The inset shows constancy of helicity flux $\Pi_H(k)$ for the wavenumber interval $21 \leqslant k \leqslant 33$, indicating an inertial range for the magnetic helicity in the direct cascade region. It can be seen in the figure that power-law scaling of $H_{mag}(k)$ extends over a larger interval, showing the scaling $H_{mag}(k) \sim k^{-3.6}$, which is in agreement with recent results on decaying 3D MHD turbulence [4]. The flux is k-dependent in the reverse spectral transfer region, as shown in the paper in the inset of Fig. 1 for the lower R_λ-run H9 and here in the inset of Fig. 5(a) for run H4a. This is also in agreement with [4], who report the same behavior. Our simulations support Kolmogorov scaling for the magnetic field as indicated by the bar parallel to $E_{mag}(k)$.

IV. EVOLUTION OF THE LOW WAVENUMBER FORM OF KINETIC ENERGY SPECTRA FOR THE FULL MHD EQUATIONS.

Figure 3 shows kinetic and magnetic energy spectra on logarithmic scales at different times during the decay for run H9, which is the run with the largest scale separation. Note that the slope of $E_{kin}(k)$ becomes flatter over time while the slope of $E_{mag}(t)$ remains the same, that is $E_{mag}(k) \sim k^4$ at small k prevails, as indicated the diagonal line superimposed above $E_{mag}(k)$ in the low wavenumber region. The slope of $E_{kin}(k)$ does *not* change from k^4 to k^2, instead it continues to flatten over time.

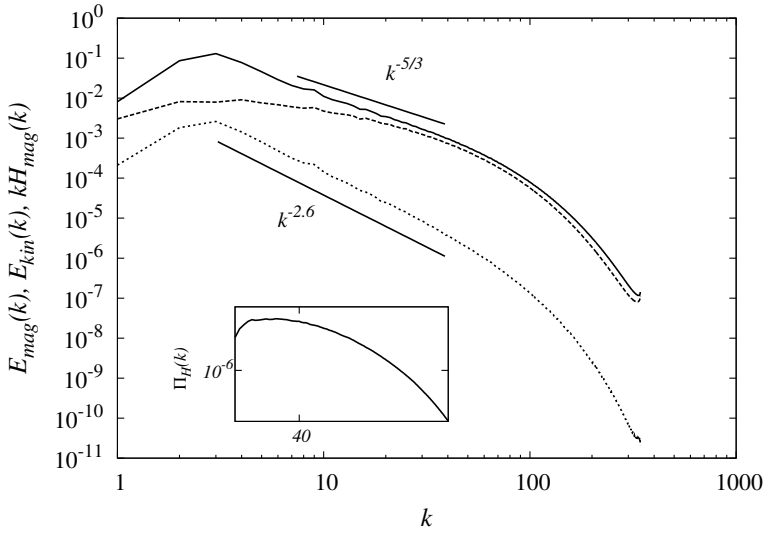


FIG. 2. Spectra for the largest Reynolds number run (H11). The solid line shows $E_{mag}(k)$, the middle dashed line shows $E_{kin}(k)$ and the bottom dotted line shows $kH_{mag}(k)$, which has been shifted for easier comparison. The inset shows the flux of $H_{mag}(k)$, which is constant in the higher k region, indicating an inertial range. The straight lines indicate scaling regions for $E_{mag}(k) \sim k^{-5/3}$ and $kH_{mag}(k) \sim k^{-2.6}$, which results in $H_{mag}(k) \sim k^{-3.6}$.

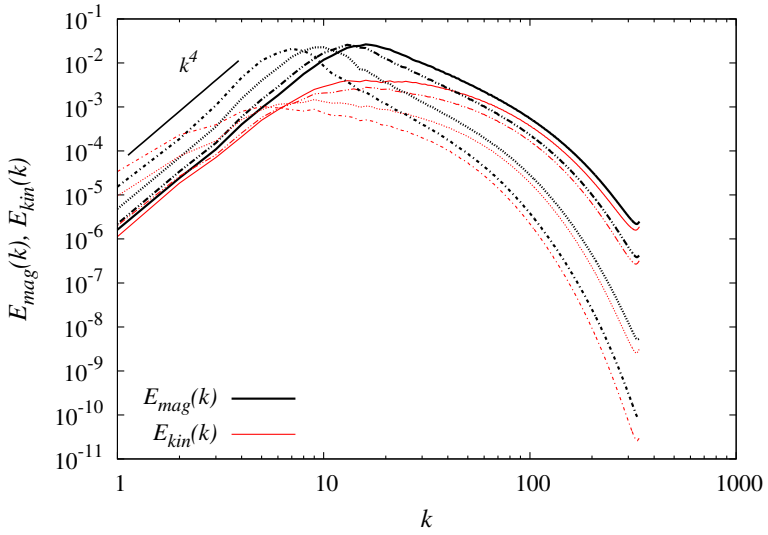
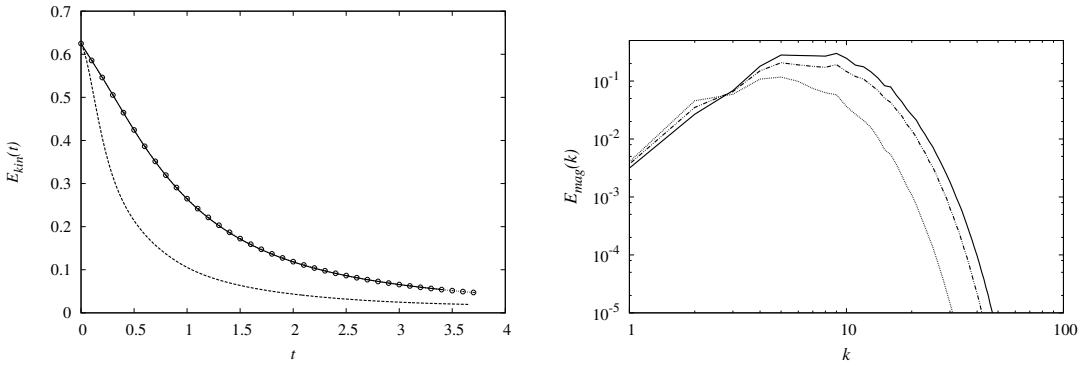
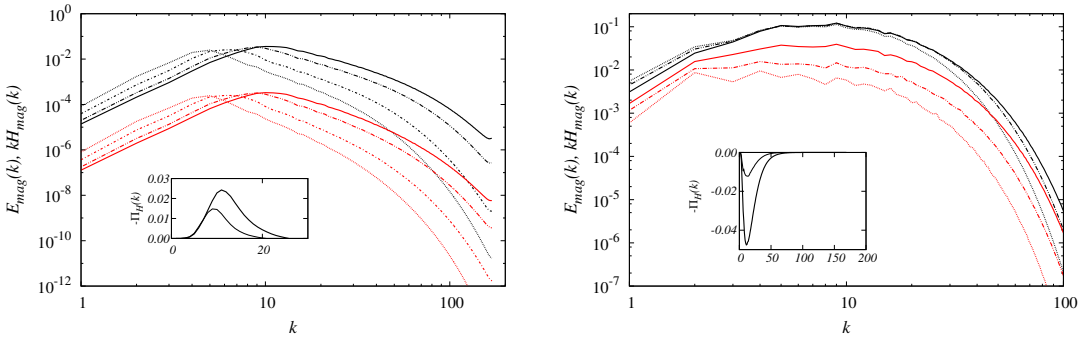


FIG. 3. (Color online) Evolution of kinetic (thin red (grey) lines) and magnetic (thick black lines) energy spectra over time for run H9. Note how the slope of $E_{kin}(k)$ flattens with time, while the slope of $E_{mag}(k)$ remains unchanged.



(a)Comparison to hydrodynamics (b)Results using the Pencil Code

FIG. 4. (a) The solid line shows $E_{kin}(t)$ from a hydrodynamic run, the symbols shows $E_{kin}(t)$ from a simulation where the momentum equation was decoupled from the induction equation, and the dashed line shows $E_{kin}(t)$ of a full MHD run. The evolution of $E_{kin}(t)$ coincides for the hydrodynamic run and the simulation of the decoupled case, showing that in the decoupled case the velocity field evolves independently of the magnetic field, as expected. (b) Linear RST of magnetic energy using the Pencil Code on 128^3 grid points.

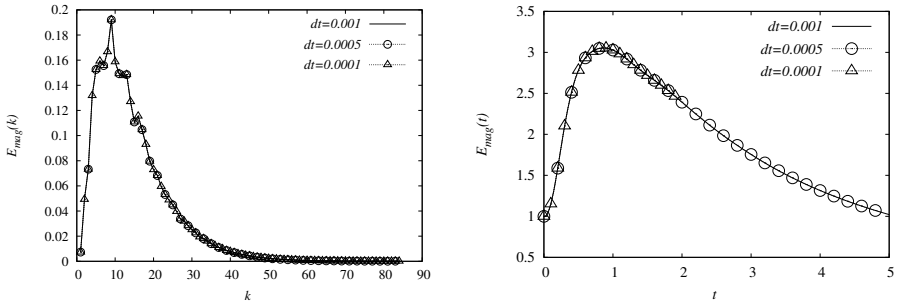


(a)Coupled case (b)Decoupled case

FIG. 5. (a) (Color online) Magnetic energy and helicity spectra showing reverse spectral transfer for a run on 512^3 grid points (H4a). The black (upper) lines refer to $E_{mag}(k)$, red (lower) lines refer to $H_{mag}(k)$. Solid lines indicate one initial large eddy turnover time, dotted and dash-dotted lines refer to 2, 5 and 10 turnover times. The inset shows the flux of magnetic helicity at one and two turnover times. (b) Magnetic energy and helicity spectra for the decoupled case on 512^3 grid points (Hd3). Upper (black) lines refer to $E_{mag}(k)$, lower (red) lines to $H_{mag}(k)$. The inset shows the flux of magnetic helicity.

V. FURTHER TESTS OF LINEAR RST

We have conducted further tests in order to validate the linear RST found in our simulations. The velocity field should evolve as in hydrodynamic turbulence if the Lorentz force term is omitted from the momentum equation. We have tested that this is the case, see Fig. 4(a), this test clearly shows that the velocity field evolves independently from the magnetic field. The



(a)Energy spectra (b)Time evolution of the magnetic energy

FIG. 6. (a) Results for magnetic energy spectra from simulations run at different time-steps on 256^3 grid points. The spectra obtained from simulations using different time-steps coincide. (b) The evolution for the magnetic energy is the same for simulations using different time-steps.

linear RST of magnetic energy was also found for slightly compressible MHD using the Pencil Code [5]. Figure 4(b) shows that after removing the Lorentz force term in the momentum equation in the Pencil Code we still observe RST of magnetic energy.

Results for the linear RST of magnetic energy were found in simulations using 256^3 up to 1032^3 collocation points, but only the highest resolved results with the largest scale separation are included in the paper [1]. Figure 5(b) shows results from simulations using 512^3 collocation points (Hd3), where the peaks of the initial spectra had been set at $k_0 = 5$. The linear RST is still visible, but concentrated at the very lowest wavenumbers. In contrast, the simulation results shown in the paper are obtained by setting the peaks of the initial spectra at $k_0 = 23$, and RST can be seen up to $k = 7$ in Fig. 3(a) of the paper. Figure 5(b) also shows that RST is absent for the magnetic helicity, as there is no increase of $H_{mag}(k)$ at the low wavenumbers and the flux of magnetic helicity is negative. For comparison, the coupled case shows RST for both $H_{mag}(k)$ and $E_{mag}(k)$ as can be seen in Fig. 5(a), where the inset shows positive flux of kinetic helicity in the low k region.

Figure 6 shows that our simulations have converged for the time-step chosen. We do not see differences in the magnetic energy spectra and the magnetic energy as we reduce the time-step, results are shown for 256^3 grid points.

VI. IMPORTANCE OF ENSEMBLE AVERAGING

A. Decay exponents

Figure 7 illustrates the importance of ensemble averaging for the measurement of the decay exponent n_E, showing all realizations of H2 and the ensemble average. It can clearly be seen how the decay exponents for single realizations differ at later times, and how they deviate from the exponent measured at early times. By contrast, the ensemble average follows the same straight line for all times after the onset of power-law decay. Similarly, a recent study of 2D hydrodynamic turbulence [6] using ensemble averaging showed a significant spread in the evolution of the integral scale for different realizations and a somewhat less pronounded spread in the total energy decay curves (see their Fig. 3). The decay exponent n_E measured from individual realizations of H2 can range from 0.81-0.96 for $t > 7t_0$, where t_0 denotes the initial large eddy turnover time.

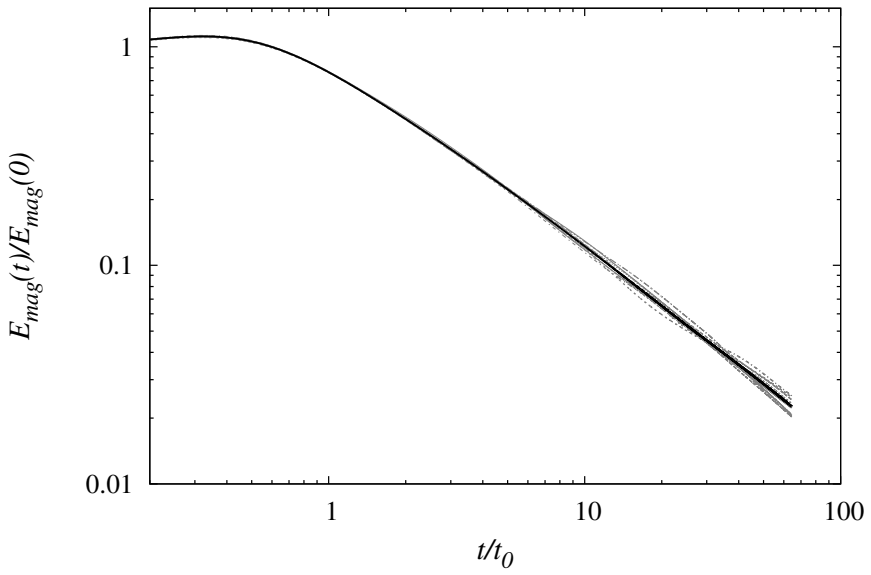


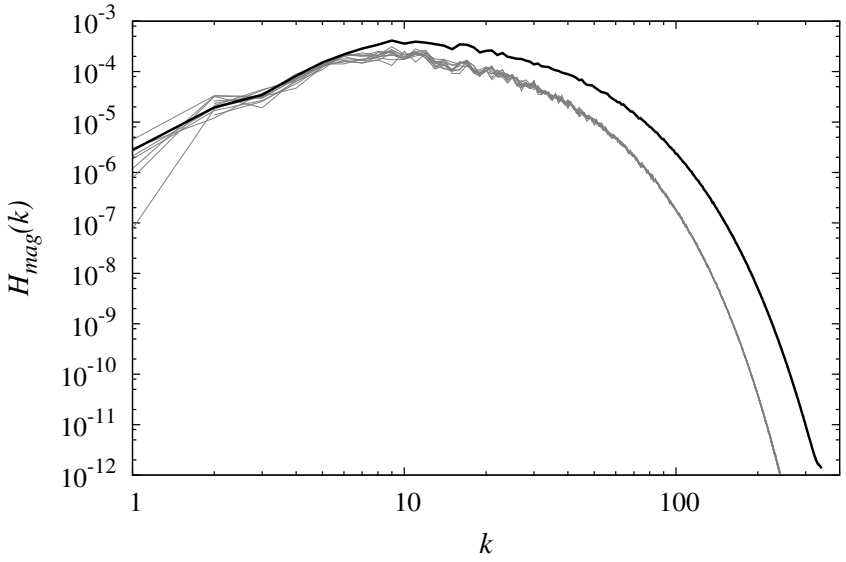
FIG. 7. Deviation of realizations (grey lines) from the ensemble average (black line) of run H2. Note that there is a clearly visible spread between realizations for $t/t_0 \geq 7$.

B. Magnetic helicity for the decoupled case

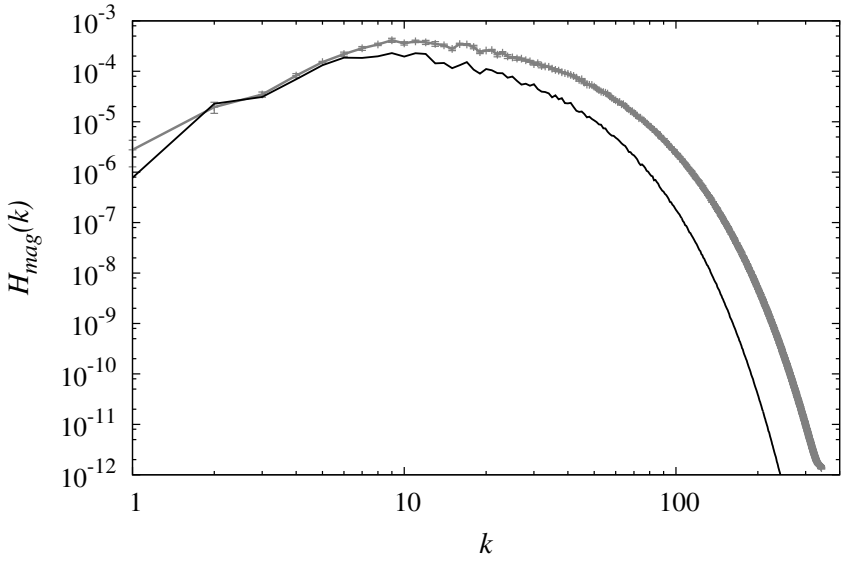
As mentioned in the paper [1], some realizations of Hd5 appeared to show RST, but the ensemble average did not confirm this. As can be seen in Fig. 8(a), the error on the ensemble averaged helicity spectrum is large at $k = 1$. Some realizations clearly show RST, some do not and some realizations show negative helicity at $k = 1$, which is why the value does not appear on a logarithmic scale.

Taking data from one realization only could have lead to erroneous results, claiming that either $H_{mag}(k)$ does show reverse spectral transfer, or that $H_{mag}(k)$ becomes negative at $k = 1$. The ensemble averaged result shows that neither is the case. For $k = 2$ there appears to be a hint of RST, but as can be seen in Fig. 8(b) the helicity spectrum at later time lies within the error of the helicity spectrum at earlier time.

We would like to thank Jorge Morales for kindly providing us with a dataset of simulation results using the Orszag-Tang vortex as initial condition.



(a)Helicity spectra of all realizations of the ensemble Hd5



(b)Ensemble averaged helicity spectra for run Hd5

FIG. 8. (a) The black line shows the ensemble average of $H_{mag}(k)$, the grey lines show $H_{mag}(k)$ for all realizations of run Hd5 at later time. Note the large deviations between realizations at low k. (b) The black line shows the ensemble average over the realizations in (a). What appears as a hint of RST at $k = 2$ lies within the error of the ensemble average at earlier time (grey line).

Run id	N^3	$k_{max}\eta_{mag}$	$R_\lambda(0)$	η	k_0	#	t_{max}/s
H1	128^3	1.30	28.69	0.009	5	10	50
H2	256^3	2.42	32.27	0.008	5	10	50
H3	256^3	2.18	36.88	0.007	5	10	50
H4	256^3	2.08	43.03	0.006	5	10	50
H5	256^3	1.80	51.64	0.005	5	10	50
H6	256^3	1.59	64.55	0.004	5	10	50
H7	256^3	1.30	86.06	0.0031	5	10	50
H4a	512^3	1.38	43.03	0.002	15	10	48
H8	512^3	2.01	129.09	0.002	5	10	7
H9	1024^3	1.38	74.84	0.00075	23	10	6
H10	528^3	1.31	258.19	0.001	5	10	50
H11	1032^3	1.38	645.47	0.0004	5	5	12
NH1	128^3	1.29	28.69	0.009	5	10	50
NH2	256^3	1.51	64.55	0.004	5	10	10
NH3	256^3	1.26	86.06	0.003	5	10	12
NH4	512^3	1.43	129.09	0.002	5	10	10
NH5	512^3	1.30	172.13	0.0015	5	10	7
Hd1	256^3	1.26	43.03	0.006	5	10	5
Hd2	256^3	1.26	43.03	0.006	5	10	5
Hd3	512^3	1.88	57.38	0.0045	5	10	5
Hd4	528^3	1.95	57.38	0.0045	5	10	5
Hd5	1032^3	1.39	28.06	0.001	23	10	2
NHd1	256^3	1.26	43.03	0.006	5	10	5
NHd2	256^3	1.26	43.03	0.006	5	10	5
NHd3	512^3	1.88	57.38	0.0045	5	10	5

TABLE I. Specifications of simulations. H refers to an initially helical magnetic field, NH to an initially non-helical magnetic field. The additional letter d refers to the decoupled system, $R_\lambda(0)$ denotes the initial Taylor-scale Reynolds number, η the magnetic resistivity, k_0 the peak wavenumber of the initial energy spectra, k_{max} the largest resolved wavenumber, η_{mag} the Kolmogrov microscale associated with the magnetic field, # the ensemble size and t_{max} the run time. The run NHd2 was started from initial spectra following k^2 at low wavenumbers k, and runs Hd2 and Hd4 were started using a maximally helical initial velocity field.

[1] A. Berera and M. F. Linkmann, (2014).
[2] P. D. Mininni, A. G. Pouquet, and D. C. Montgomery, Phys. Rev. Lett., **97**, 244503 (2006).
[3] J. A. Morales, M. Leroy, W. J. T. Bos, and K. Schneider, J. Comp. Phys., **274**, 64 (2014).
[4] W. C. Müller, S. K. Malapaka, and A. Busse, Phys. Rev. E, **85**, 015302 (2012).
[5] `http://pencil-code.googlecode.com/`.
[6] P. D. Mininni and A. Pouquet, Phys. Rev. E, **87**, 033002 (2013).